



A new intranuclear microsporidium, *Enterospora nucleophila* n. sp., causing an emaciative syndrome in a piscine host (*Sparus aurata*), prompts the redescription of the family Enterocytozoonidae [☆]



Oswaldo Palenzuela ^{a,1}, María José Redondo ^{a,1}, Ann Cali ^b, Peter M. Takvorian ^b, María Alonso-Naveiro ^a, Pilar Alvarez-Pellitero ^a, Ariadna Sitjà-Bobadilla ^{a,*}

^a Fish Pathology Group, Instituto de Acuicultura Torre de la Sal, Consejo Superior de Investigaciones Científicas (IATS-CSIC), 12595 Ribera de Cabanes, Castellón, Spain

^b Dept. of Biological Sciences, Rutgers University, 195 University Avenue, Newark, NJ 07102, USA

ARTICLE INFO

Article history:

Received 16 August 2013

Received in revised form 24 October 2013

Accepted 25 October 2013

Available online 8 December 2013

Keywords:

Fungi

Rodlet cells

Enterocytes

Ultrastructure

Molecular phylogeny

Pathology

Fish

Intestine

ABSTRACT

The presence of a new microsporidium is believed to be responsible for an emaciative syndrome observed in farmed gilthead sea bream (*Sparus aurata*) from different facilities along the Spanish coast. Infected fish were approximately half the average weight and significant mortality was attributed to the condition in some facilities. Clinical signs included anorexia, cachexia and pale internal organs. The microsporidium was found mainly in the intestinal mucosa and occasionally in the submucosa. Morphological, histopathological, ultrastructural and molecular phylogenetic studies were conducted to characterise this organism. This microsporidium undergoes intranuclear development in rodlet cells and enterocytes, and cytoplasmic development mainly in enterocytes and macrophages. The nucleus-infecting plasmodium contains several diplokarya and displays polysporous development which occurs without an interfacial envelope. In the host cell cytoplasm, the parasite develops within a membrane-bound matrix. In both infection locations, the polar tube precursors appear as disks, first with lucent centres, then as fully dense disks as they fuse to form the polar filament, all before division of the plasmodium into sporoblasts. Up to 16 intranuclear spores result from the sporogonic development of a single plasmodium, whereas more than 40 spores result from several asynchronous reproductive cycles in the cytoplasmic infection. Fixed spores are ellipsoidal and diplokaryotic, with five to six coils of an isofilar polar filament in a single row. ssrDNA-based molecular phylogenetic inference places this parasite as a sister clade to crustacean-infecting species of the Enterocytozoonidae and closer to *Enterocytozoon bieneusi* than to other fish-infecting microsporidians presenting intranuclear development, i.e. *Nucleospora*, *Paranucleospora* and *Desmozoon*. Our studies result in the erection of a new species, *Enterospora nucleophila*, within the family Enterocytozoonidae, and the description of this family is amended accordingly to accommodate the features of known species assigned to it. Severe histopathological damage occurs in intense infections and this microsporidian is considered a serious emerging threat in sea bream production.

© 2013 Australian Society for Parasitology Inc. Published by Elsevier Ltd. All rights reserved.

1. Introduction

Microsporidia are unicellular eukaryotes living as obligate intracellular parasites in a variety of hosts, from invertebrates to humans. Infections in insects and fish have been reported for over a hundred years but it was not until the 1970s that human infections became known. Microsporidiosis occurs both in immunosuppressed and immunocompetent patients, producing sub-clinical to lethal infections (Didier and Weiss, 2011). Microsporidia causing disease

or having an economic impact in aquaculture and ornamental fish were reviewed by Lom (2002) and some are considered a potential threat for fish populations, e.g., in the Red Sea (Abdel-Ghaffar et al., 2011). Several microsporidian species have been described in wild and cultured gilthead sea bream (Faye et al., 1990; Mathieu-Daudé et al., 1992; Abela et al., 1996; Athanassopoulou, 1998), but none of them are intranuclear, or infect the intestinal epithelium. Additionally, most of them produce xenomas in muscle. The taxonomy and phylogeny of microsporidians have undergone much revision in recent years. Although traditionally included with the Protozoa, or as Protists related to the Fungi, some studies have placed them within the Fungi or as a sister group to these, i.e., sharing a common ancestor (Gill and Fast, 2006; Lee et al., 2008). Within the described species in this diverse phylum, to date only a few species have been

[☆] Nucleotide sequence data generated in this study are available in GenBank under Accession numbers JX101917 and KF135641–KF135645.

* Corresponding author. Tel.: +34 964319500; fax: +34 964319509.

E-mail address: ariadna.sitja@csic.es (A. Sitjà-Bobadilla).

¹ These authors made equal contributions to this article.

reported to have intranuclear development, and currently those infections are exclusively from fish or crustaceans. These are: *Microsporidium rhabdophilia* (Modin, 1981), *Nucleospora salmonis* (Hedrick et al., 1991), *Nucleospora secunda* (Lom and Dyková, 2002), *Nucleospora cyclopteri* (Mullins et al., 1994; Freeman et al., 2013), *Enterospora canceri* (Stentiford et al., 2007) and *Paranucleospora theridion* (Nylund et al., 2010). The latter species is now considered a synonym of *Desmozoon lepeophtherii* (Freeman et al., 2003; Freeman and Sommerville, 2009) based on their molecular identity (Freeman and Sommerville, 2011; Nylund et al., 2011). In addition, intranuclear development has been described in putative *Nucleospora* spp. from fish lymphocytes (Nilsen et al., 1995), and in inflammatory cells in English sole (*Pleuronectes vetulus*) X-cell pseudotumours (Gresoviac et al., 2007).

Molecular phylogenetic studies of some of these intranuclear microsporidians suggest that they are related to the human parasite *Enterocytozoon bieneusi*, and thus they are included in the family Enterocytozoonidae (Vossbrinck and Debrunner-Vossbrinck, 2005). Additional organisms presenting cytoplasmatic development, such as *Hepatospora* spp. from crabs (Stentiford et al., 2011) and *Enterocytozoon* sp. from black tiger prawn (Tourtip et al., 2009), as well as some uncharacterised genotypes from freshwater crustaceans such as cladocerans (e.g., Refardt et al., 2002) or amphipods (GenBank Accession No. FJ756170) can also be grouped within, or related to, this family.

The present study focused on the characterisation of the etiological agent responsible for an emaciative syndrome affecting gilthead sea bream, *Sparus aurata*, a marine teleostean extensively cultured in the Mediterranean basin. A new intestinal microsporidium was found associated with this disease and it is described on the basis of biological, epidemiological, morphological, ultrastructural and molecular data, obtained from more than a decade of monitoring disease episodes affecting several sea bream farms. In view of the features of this new microsporidian species and the available information from other genera and species, an amended description of the family Enterocytozoonidae is proposed.

2. Materials and methods

2.1. Fish and sampling procedure

Gilthead sea bream samples were obtained from different farming facilities located in Spain. Data on the fish examined, location and type of facility are shown in Table 1. Fish were necropsied in situ by the fish farm staff or sent alive to the facilities of the Instituto de Acuicultura Torre de la Sal (IATS-CSIC) Spain. In all cases, fish were sacrificed by overexposure to anaesthetic followed by severing of the spine. Pieces of intestine (the target tissue of this

microsporidium) of each fish were fixed in 10% buffered formalin for histology and, when possible, parallel samples were fixed in 2.5% (v/v) glutaraldehyde in 0.1 M cacodylate buffer (pH 7.2) at 4 °C for transmission electron microscopy (TEM) and in absolute ethanol for DNA extraction. The latter two types of samples were kept at 4 °C until use. In some cases, additional samples from other organs (viscera, muscles and gills) were taken during parasitological surveys.

Necropsies performed at IATS were carried out in accordance with the principles published in the European animal directive (86/609/EEC) for the protection of experimental animals and in compliance with national laws (Royal Decree RD1201/2005) for the protection of animals used in scientific experiments, and approved by the Consejo Superior de Investigaciones Científicas (CSIC) ethics committee and IATS Review Board.

2.2. Light and transmission electron microscopy and histology

Fixed intestine samples were embedded in paraffin or Technovit 7100 resin (Heraeus Kulzer, Wehrheim, Germany) using standard histological procedures. Paraffin sections (4 µm) were stained with H&E or with Giemsa's stain, and plastic sections (1 µm) were stained with toluidine blue (TB), periodic acid-schiff (PAS) Luna's or Giemsa's stain. In addition, some paraffin samples were stained with Calcofluor-white or Uvitex 2B whiteners (0.1% w/v in ddH₂O) and observed using an epifluorescence microscope under UV light. Intensity of infection was semi-quantitatively evaluated using a conventional scale from 1+ to 6+, according to the relative numbers of parasites present in each microscopic field at 320×. For specimens diagnosed as microsporidium-positive by light microscopy, parallel samples fixed for TEM were post-fixed in 1% OsO₄, dehydrated through a graded ethanol series and embedded in Spurr's or Lowicryl resins. Ultrathin sections (60–90 nm) were stained with uranyl acetate and lead citrate, and observed with a Jeol-1010 or a FEI Techni 12 TEM, operating at 60–70 or 80–100 kV, respectively.

2.3. DNA isolation, cloning and sequencing

Ethanol-preserved intestines from selected fish, diagnosed as heavily infected in the histopathological and TEM examinations, were used. The samples used corresponded to two individual fish selected from farms B and D (Table 1), harbouring stages predominantly in intranuclear and cytoplasmatic location, respectively. Genomic DNA was extracted using a silica-based commercial kit (Roche Applied Science, Barcelona, Spain). Control DNA was also extracted from healthy juvenile sea bream. Taxon-specific primers targeting the ssrDNA of microsporidians, ss18f and ss1492r (Ghosh

Table 1
Facilities sampled for gilthead sea bream (*Sparus aurata*), with details of infection with *Enterospora nucleophila*. A prior case was detected in June 1993 in farm B but, since all of the epidemiological data are not available, it is not included here.

Fish farm ^a	Type of facility	Sampling date	No. fish examined	Mean weight (g) ^b	Prevalence (%)	Mean intensity	Clinical signs
A	Sea cages	July 2000	20	339.8	5	5+	Whitish faeces
B	Concrete ponds	June 2006	20	55.7	80	2.5+	Poor growth
	Earth ponds	September 2006	20	15	5	1+	None
	Earth ponds	September 2007	10	182.7	10	3.5+	None
C	Sea cages	November–December 2007	44	109.1	10	2.3+	Poor growth, mortalities
D	Sea cages	March 2011	5	20 (46)	80	3.75+	Poor growth, mortalities
			4	200–250	50	2.5+	
			10	45	50	1+	
			10	25	60	2.7+	
		May 2011	8	60 (120)	12.5	3+	Anorexia, poor growth
			2	25 (90)	50	1+	

^a All farms with sea cages were located off the Spanish Mediterranean coast. Farm B was located in the southern Atlantic Spanish coast.

^b Values in brackets indicate the expected mean value determined by fish farmers according to previous biometrical records, when available.

and Weiss, 2009) were used in the PCRs. Each reaction (50 µl) contained 1× Taq buffer with 2 mM MgCl₂, 0.2 mM each deoxyribonucleotide triphosphate (dNTP), 1 U Taq DNA polymerase and 25 pmol of each primer. Cycling conditions consisted of an initial denaturation (2 min at 94 °C) and 35 amplification cycles (94 °C for 30 s, 55 °C for 30 s, 72 °C for 75 s) followed by a final 10 min incubation at 72 °C.

Amplification products were analysed on Tris-acetate-EDTA agarose gels and amplicons were cloned or used directly for automated sequencing. For cloning, fresh PCR products were ligated into a plasmid vector (PCR4-TOPO, Invitrogen, USA), which was used to transform competent *Escherichia coli*. Transformants were selected on Lennox L Agar (LB-agar) plates and plasmids were purified from overnight cultures in liquid media. The presence of the inserts of the expected size was confirmed by restriction digestion analysis with EcoRI enzyme. Both strands of cloned products were sequenced using M13F and M13R primers.

2.4. Phylogenetic analysis

DNA sequences were assembled and edited using the MacVector software package (Rastogi, 2000). Homologous positions presenting differences between contigs were detected and verified by manual inspection of the electropherograms. Consensus sequences were used as queries in the NCBI GenBank database using BLASTn (Altschul et al., 1990) to identify the most closely related organisms. The final, proofed sequences were inserted in an alignment of 1,621 sequences available under the category "Microsporidia" (123 "Enterocytozoonidae") in the SSU_r114 database release (February 2013) by SILVA (Pruesse et al., 2007; <http://www.arb-silva.de>). The alignment was refined manually using ARB software (Ludwig et al., 2004) according to secondary structure criteria and the dataset was pruned to a selection of the longest, best quality sequences available from the closest relevant taxa. Unambiguously aligned positions were sampled for phylogenetic inference using different methods and substitution models with MEGA v.5.0 software (Tamura et al., 2011). Bayesian phylogenetic inference was conducted with MrBayes (Huelsenbeck and Ronquist, 2001; Ronquist and Huelsenbeck, 2003), under the EPoS software framework (Griebel et al., 2008).

3. Results

3.1. Clinical signs, epidemiology, light microscopy and histopathology

The most common clinical manifestation associated with microsporidiosis in gilthead sea bream facilities was stunted growth and trickling mortality in fish during their first winter in sea cages. Infected fish exhibited cachexia, emaciation and lethargy, with occasional scale loss and were approximately half the estimated average weight (Fig. 1). Mortality attributed to this condition was quite variable, with farm reports of a daily mortality of approximately 0.1–0.3% per cage (up to 1% during peaks) and sustained throughout the winter. At necropsy, internal organs appeared pale but no gross pathological alterations were noticed. Other parasites were also detected in microsporidium-infected fish, sometimes also in the intestine, such as the myxozoan *Enteromyxum leei* or the apicomplexan *Cryptosporidium molnari*, but their prevalence and intensity did not explain the condition. Table 1 shows the prevalence of the microsporidian infection in the sampled facilities under different rearing conditions.

Microscopic identification of low intensity infections was often overlooked due to the minute spore size of the microsporidium and their sparsity in host tissue. However, in heavy infections spores could be observed, even in fresh smears (Fig. 2A). Additionally, in



Fig. 1. *Sparus aurata* (B) with typical reduced growth due to *Enterospaera nucleophila* compared with a non-affected fish (A) of the same age and entrance time in the cage.

histological sections of the intestinal epithelium of heavily infected fish, numerous cells with hypertrophied nuclei and an overall hypercellularity were noticed at low magnification. In Calcofluor-White-stained sections, numerous fluorescent-stained infected cells were detectable at low magnification (Fig. 2B). The parasite was present in two cellular locations, the nucleus or the cytoplasm (Fig. 2C).

Intranuclear infections affected enterocytes (Fig. 2D) and rodlet cells (RCs). The latter were seemingly the preferred target for the parasite, appearing in extremely high numbers (Fig. 2E), even in the intestinal submucosa (Fig. 2F), and largely contributing to an overall aspect of hypercellularity of infected epithelia. Observation of TB or Giemsa-stained histological sections revealed the presence of developmental stages within the nuclei of infected host cells (Fig. 2G). Mature spores were PAS-positive and stained red with Luna's stain (Fig. 2H). Initially, the parasite appeared as a central drop-like inclusion in the host cell nuclei, occupying one-fourth of the area (Fig. 2D). As development progressed, a plasmodium with multiple nuclei was visible (Fig. 2I) and the host nuclei appeared as peripheral rims (Fig. 2G, I). Subsequently, a rosette-like structure formed (Fig. 2J) in which plasmotomy started, followed by the appearance of sporoblasts and immature spores (Fig. 2I, K) and eventually mature spores (Fig. 2L). Clusters of spores within infected host nuclei were tightly packed, especially in RCs (Fig. 2C, E, L), in which spores appeared more compacted than in enterocytes. Up to 16 spores could be observed in a single nuclear section, but in fluorescent-stained infected cells up to 25 spores could be counted. The infection was rarely identified in the stomach, both in the epithelium and in the glandular zone. The nucleus of some leucocyte-like cells within blood vessels of the intestinal submucosa occasionally contained parasite stages.

Cytoplasmic infections were found mainly in enterocytes and in phagocytes located in the epithelium, in the lamina propria submucosa (Fig. 2F, M, N), and sometimes in melanomacrophage centres (MMCs) (Fig. 2N). Infected cells were hypertrophied and often appeared to have a thickened plasma membrane which was interpreted as remnants of condensed cytoplasm attached to the membrane (Fig. 2C, Q). Asynchronous development was obvious in these cytoplasmic stages. Spores were occasionally detected within eosinophilic cells (Fig. 2O) and within entero-endocrine cells (Fig. 2P). Few isolated spores were observed attached to the microvilli of uninfected enterocytes (Fig. 2R).

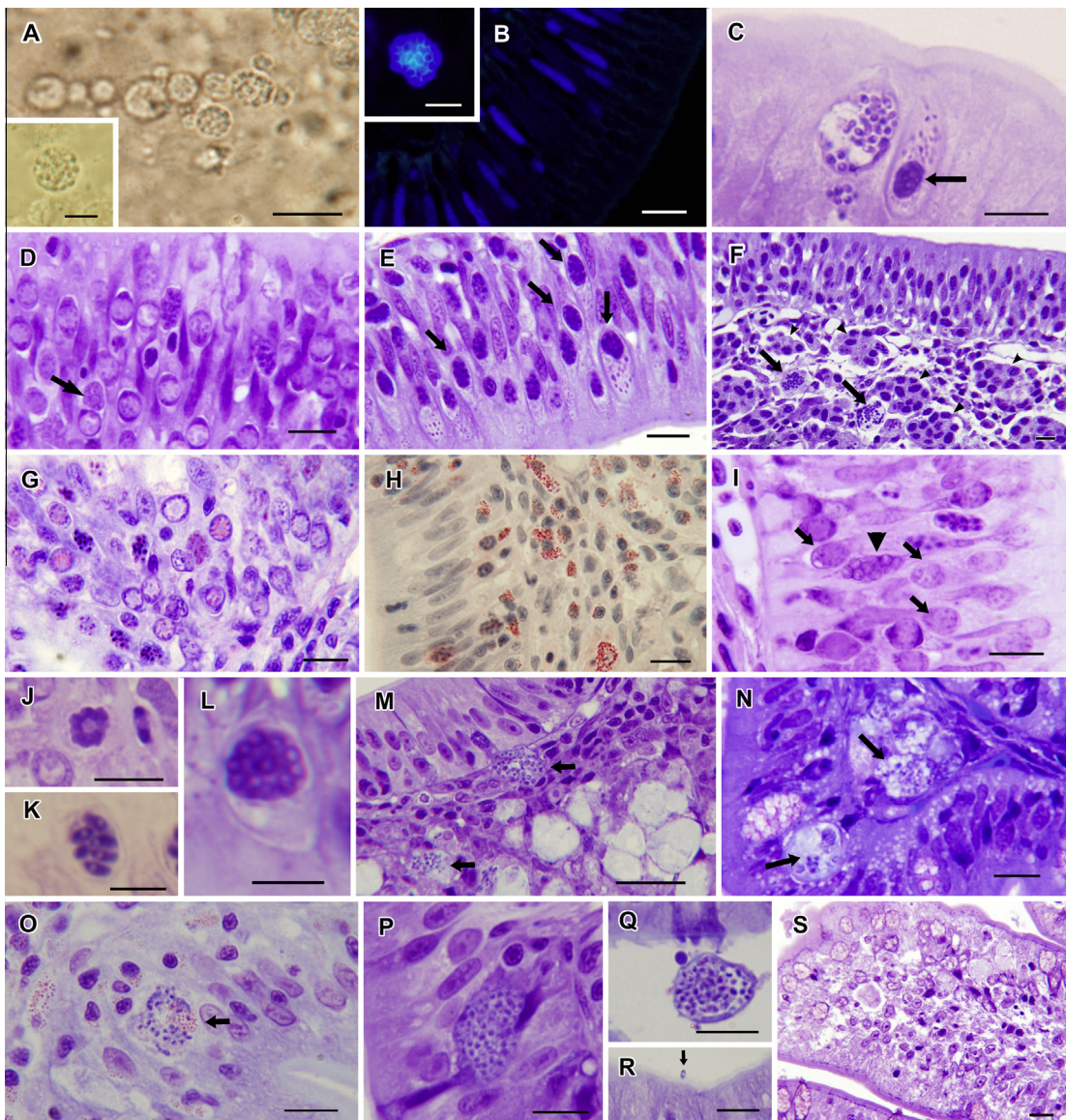


Fig. 2. Photomicrographs of *Enterospora nucleophila* from fresh smear (A) and histological sections (B–S) of the intestine of *Sparus aurata*. (A) Groups of spores. Inset: higher magnification of an infected cell. (B) Infected nuclei stained with the fluorescent brightener Uvitex-2B. Inset: detail of a group of spores. (C) Intranuclear (arrow) and cytoplasmic infection. (D) Extensive intranuclear infection of enterocytes. Note the nuclei of cells as a peripheral rim and the very early developmental stages of the microsporidian in the centre as a drop-like inclusion (arrow). (E) Severe nuclear infection of rodlet cells in the epithelial layer; arrows point to some of the nuclei packed with spores. (F) Heavy intranuclear infection of rodlet cells in the epithelium and the submucosa (arrowheads) and cytoplasmic infection in the submucosa (arrows). (G) Differential staining of plasmodial and sporogonial stages in intranuclear infections. (H) Spores and granulocytes proliferating in the submucosa are red with Luna's stain. (I) Plasmodia (arrows) and sporoblasts (arrowhead). (J) Rosette-like plasmodium. (K) Almost mature spores in longitudinal section. (L) Spores in a transverse section of an infected nucleus. (M) Spores in a cytoplasmic infection in the submucosa (arrows). Notice the presence of melanomacrophage centers. (N) Vacuolated cells and macrophages with cell debris and spores in the epithelium and submucosa (arrows). (O) Cytoplasmic infection in a granulocytic cell (arrow). (P) Cytoplasmic infection in an enteroendocrine cell. (Q) Infected cell detached from the lumen. (R) Spore attached to the brush border (arrow). (S) General vacuolisation of the intestinal epithelium after a massive infection. Stains: toluidine blue (C–F, I–S), Giemsa (G), Luna stain (H). Scale bar: A–J, M–S, B inset = 10 µm; A inset, K, L = 5 µm.

In intense advanced infections, degeneration of the intestinal epithelium was evident (Fig. 2S), goblet cells were scarce, and ruptured enterocytes and RCs containing parasite stages were shed into the intestinal lumen (Fig. 2Q). Cellular reaction in infected epithelia consisted mainly of the infiltration of eosinophilic cells that sometimes discharged their contents (Fig. 2O) when in the vicinity of parasite stages. In addition, the submucosa was hyperplastic with proliferation of eosinophilic cells (Fig. 2H) which were highlighted with Luna's stain and displayed abundant MMCs. Free spores were observed in the intestinal lumen, sometimes mixed with bacteria. In fish that overcame the disease or with terminal infections, spores were often observed within vacuolated cell debris or within MMCs (Fig. 2N). Spores from histological sections measured

$1.67 \times 1.05 \mu\text{m}$ ($n = 30$, SD = 0×0.1). Occasionally, some larger spores were observed in cytoplasmic infections. Since they were never found in TEM sections, they were considered abortive spores without further relevance.

3.2. Ultrastructure

3.2.1. Intranuclear development

The intranuclear stages were observed most often in RCs but also in enterocytes and leucocyte-like cells. In all nuclear infections the parasites were in the nucleoplasm without any membranous interface. The earliest stages observed were dense bodies in RCs (Fig. 3A), followed by early sporogonial plasmodia containing

multiple abutting nuclei arranged as diplokarya (**Fig. 3B**). Nuclei in diplokaryon arrangement were oval, with closely apposed double nuclear membranes (**Fig. 3C, D**). Host nuclear heterochromatin was attached to the plasmoidal plasmalemma (**Fig. 3B, C, F**). The

plasmodium contained abundant ribosomes and round to oval, electron-dense disks (EDDs) of two types, first with an electron-lucent core, then with a dense core, as development progressed (**Fig. 3E, F, G**). They were distributed in clusters within the

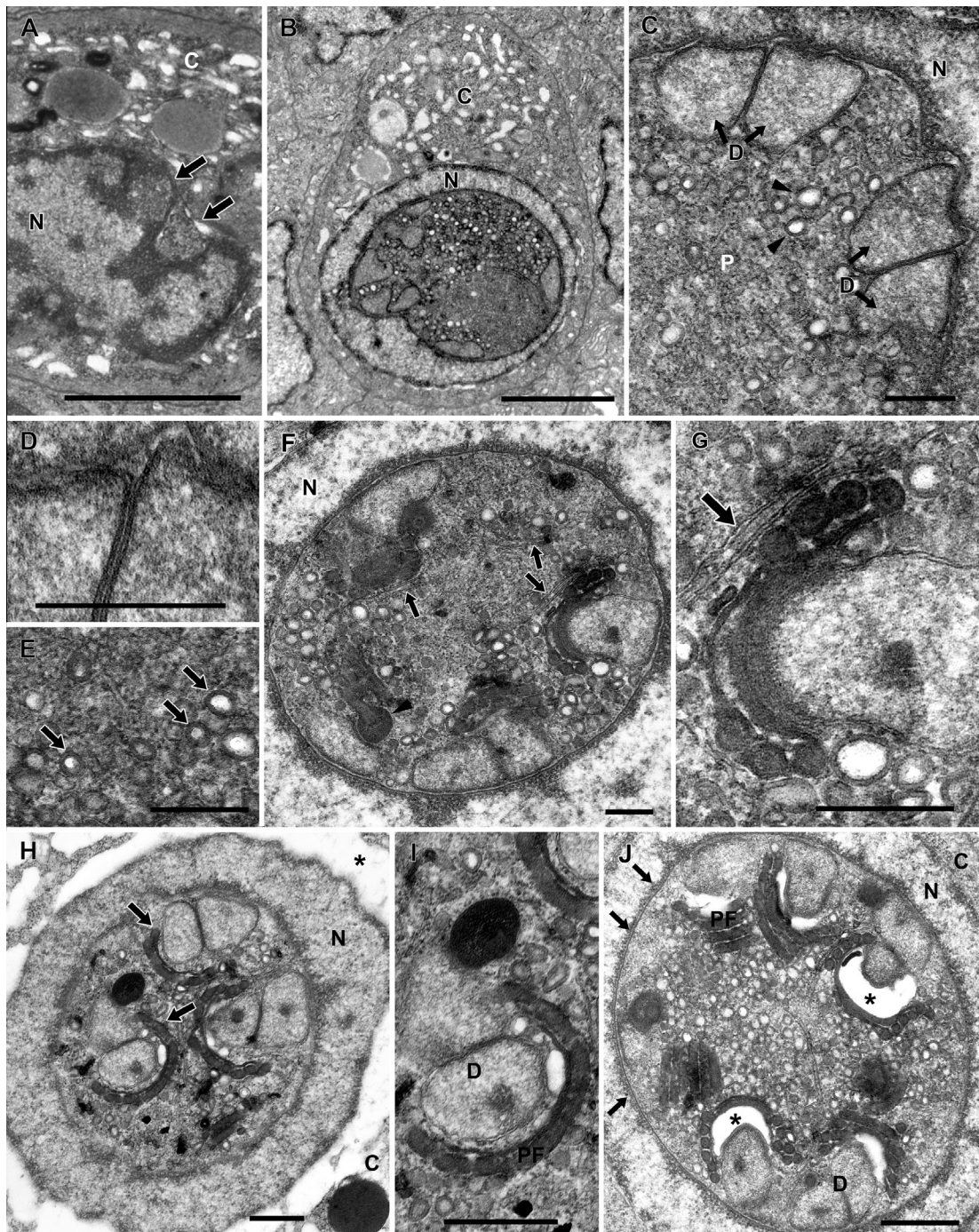


Fig. 3. Transmission electron micrographs showing the ultrastructure of intranuclear stages of *Enterospora nucleophila* in rodlet cells of the intestine of *Sparus aurata*. (A) Very early stages within the nucleoplasm (arrows) of the host nucleus (N). (B) Early sporogonial plasmodium within the host nucleus; the cytoplasm of the rodlet cells shows no pathological changes. (C) Typical diplokaryotic nuclei (arrows) of a plasmodium. Arrowheads point to some electron-dense disks. (D) Detail of the two pairs of nuclear membranes of a diplokaryon. (E) Detail of abundant electron-dense disks (arrows) and ribosomes of the plasmodium. (F) More advanced plasmodium in which the precursors of the extrusion apparatus are starting to organise around each diplokaryon. Note the abundant rough Endoplasmic Reticulum (arrows), the differentiation of the polar filament and the anchoring disk complex (arrowhead), and the host heterochromatin apposed to the plasmodium plasmalemma. (G) Detail of the electron-dense disks assembled to form the polar filament around the parasite nuclear pair and the surrounding Endoplasmic Reticulum (arrow). (H) More advanced plasmodium. Note the segments of fusing electron-dense disks forming the arched polar filaments (arrows) by each diplokaryon and the empty spaces in the cytoplasm of rodlet cells (*). (I) Higher magnification of the formation of the polar filament and the increase in Electron lucent inclusions. (J) Sporogonial plasmodium with continued enlargement of Electron lucent inclusions (*) abutting each diplokaryon, while polar filament formation is progressing. Arrows point to the host chromatin apposed to the plasmodium membrane. Scales bars: F, G = 250 nm; H, I = 300 nm; C–E = 400 nm; J = 500 nm; A, B = 2,000 nm. C, host cytoplasm; D, diplokaryotic nuclei; N, host nucleus; P, plasmodium, PF, polar filament.

plasmodium (Fig. 3C, E). As sporogony proceeded, the diplokaryotic nuclei were located at the periphery of the plasmodium with these nuclear pairs appearing to be organising centres around which were the developing polar filaments and spore forming complexes (Fig. 3C, F). Long strands of rough endoplasmic reticulum (rER) were visible surrounding these polar filament-organising centres, which separated the multiple sporoblast developing complexes (Fig. 3F, G). Eventually, the EDDs aligned and fused forming the polar filaments, each with a diplokaryon (Fig. 3H, I). Electron lucent inclusions (ELIs) were also observed between the forming polar filament and the diplokarya (Fig. 3J). When the plasmodial cell division occurred, the polar filament complexes were already well developed and the resulting sporoblasts with their polar filament, diplokaryotic nuclei and the primordial polaroplast were present in the host nucleoplasm (Fig. 4A). Early sporoblasts contained an almost fully developed polar filament (containing a dense core), the forming lamellar and vesicular polaroplast, and the diplokaryon (Fig. 4B). As sporoblasts continued their development, the two regions (outer dense lamellar and inner vesicular) of the polaroplast became evident and the cytoplasmic density increased (Fig. 4C). Late sporoblasts were characterised by an increased density of the cytoplasm, the presence of polyribosomes and the onset of spore wall formation (Fig. 4D, E). Maturing spores contained a thick electron lucent endospore wall surrounded by a thin dense exospore coat, which appeared contiguous with host heterochromatin. Polyribosomes arranged in belts around the polaroplast and the diplokaryon were also present (Fig. 4F).

Mature spores (Fig. 4G), displayed the typical spore wall of the Microsporidia, with a dense exospore coat (22.8 ± 5.7 nm thick) surrounding a thick electron lucent endospore (44.5 ± 10.6 nm thick) and the plasma membrane (Fig. 4H). Host heterochromatin remained attached to the exospore layer and surrounding parasite stages (Fig. 4G, H). The polar filament, with 5–6 turns in a single row, was of the isofilar type, with a diameter of 71.6 ± 4 nm (Fig. 4I). At the anterior end of the spore, there was an anchoring disk to which the polar filament attached. The manubroid portion of the polar filament was surrounded by the vesicular and lamellar polaroplast (Fig. 4J). The polaroplast was round and elongated, with a peripheral dense lamellar part surrounding a less dense vesicular region (Fig. 4K, L). An electron lucent vacuole was sometimes visible at the posterior part of the spore. Sporogenesis in the host nuclei was synchronous and a single cluster of spores was formed within each nucleus, the highest number of spores observed in a thin section being 13.

Infected RCs kept their sub-plasmalemmal capsule in most cases and the cytoplasm was rich in mitochondria, Golgi cisternae, vesicles and ribosomes, especially close to the nuclear membrane. The most conspicuous effects of the infection on a RC were the low number of rods, the intense vacuolisation of the cytoplasm and occasionally the presence of myelinic structures (Fig. 4M). In addition, the intercellular space between RCs appeared highly vacuolated and necrotic.

3.2.2. Cytoplasmic development

The earliest stages in the host cytoplasm were small, round and uniformly dense merogonial plasmodia of approximately $0.9\text{ }\mu\text{m}$ (Fig. 5A). Larger merogonial (proliferative) plasmodia also contained diplokaryotic nuclei (Fig. 5B). Early sporogonial plasmodia had very similar ultrastructural features to those found in the intranuclear infection: both had diplokaryotic nuclei and precocious polar filament formation (Fig. 5A–C). However, all of the cytoplasmic stages (merogonial and sporogonial plasmodia, sporoblasts and spores) developed in a dense matrix of variable appearance (Fig. 5A, C, E, J), surrounded by an interfacial envelope (Fig. 5C–E, I, J). The envelope often abutted the host nucleus (Fig. 5C, D, I). Host mitochondria and endoplasmic reticulum (ER)

were occasionally observed in close contact with the parasite stages (Fig. 5A, D, H). Sporogonial plasmodia divided, producing sporoblasts, each containing a diplokaryon and polar filament complex (Fig. 5H, I). As these sporoblasts matured and the spore coat developed, their cytoplasm increased in density (Fig. 5I). Mature spores were usually interspersed with electron-dense material (Fig. 5G, K). A single section of an infected host cell contained more than 40 spores (Fig. 5K) and it could harbour several plasmodia in asynchronous development (Fig. 5G, J). Occasionally the cytoplasm of infected cells appeared vacuolated. Macrophages contained mature or effete spores depending on the stage of the infection (Fig. 5K).

No cell was observed to be infected in both the nucleus and in the cytoplasm simultaneously. Spore measurements in nuclear and cytoplasmic locations were not statistically different ($P < 0.05$) and the resulting pooled values were $1.83 \pm 0.15 \times 1.11 \pm 0.15\text{ }\mu\text{m}$. Diagrammatic interpretations of the intranuclear and cytoplasmic developmental patterns are summarised in Fig. 6.

3.3. Molecular phylogeny

The PCR using microsporidian-specific primers amplified a ≈ 1.3 Kb DNA fragment in most samples histologically diagnosed as heavily positive for the microsporidian. This DNA fragment was not present in uninfected (control) sea bream. The products obtained from two different fish were cloned and sequenced entirely. The consensus sequence (1,298 bp) was identified as a Microsporidian ssrDNA and the closest relatives identified in BLAST searches (highest 'S score' values) were complete ssrDNA sequences of *En. bieneusi* ($S = 1,501$) and *N. salmonis* ($S = 1,431$). When filtering out short sequences from the NCBI database (<400 bp), the highest pairwise identity values matched partial sequences of *Enterocytozoon* sp. from black tiger shrimps (89.6% identity along 857 sites, $S = 1,123$) and *E. canceri* from European crabs (87.2% along 835 sites, $S = 1,024$). Six clones were sequenced entirely, two from farm B (NUC isolates) and four from farm D (ENT isolates). Minor variations between the clones identified six haplotypes (99.6% pairwise identity and 98.8% identical sites). The mean distance (in base differences) between clones from farms B and D was 5 ($n = 6$) whereas the differences within each sample were 6 and 4, respectively.

Considering only the Enterocytozoonidae with long ($>1,100$ bp), high quality sequences available in public databases, the Enterocytozoonidae were resolved as two well-supported subclades: one of them grouping *Nucleospora* spp. and *P. theridion/D. lepeophtherii*; and a second subclade including *En. bieneusi* (Fig. 7). In these analyses, the genotypes from the gilthead sea bream microsporidium (GSBM) were resolved as a sister taxon to *En. bieneusi*, and this basic topology was robustly supported using different inference methods and substitution models (Fig. 7 and data not shown). Inclusion of the recently described genus *Hepatospora*, with two partial sequences available (957 and 612 bp), and of additional, putative Enterocytozoonidae sequences yielding high scores in the BLAST search, resulted in additional independent lineages accommodating *Hepatospora* spp. and a genotype (*Microsporidium* sp. MIC-2) from *Daphnia* (Fig. 8). The gilthead sea bream genotypes were resolved as a sister clade with *Enterocytozoon hepatopenaei*, a recently described species from black tiger shrimp (BTSM), with very high bootstrap support under all of the conditions tested. Other partial sequences clustering within this Enterocytozoonidae subclade included an uncharacterised genotype, "Microsporidium" sp. BVER-2", from *Eulimnogammarus verrucosus* (GenBank Accession No. FJ756170), as well as *E. canceri* from European crabs (Fig. 8). As a result of the limited overlapping length and the poor quality of some of these sequences, the bootstrap support for secondary nodes in trees containing all of them was low and their position

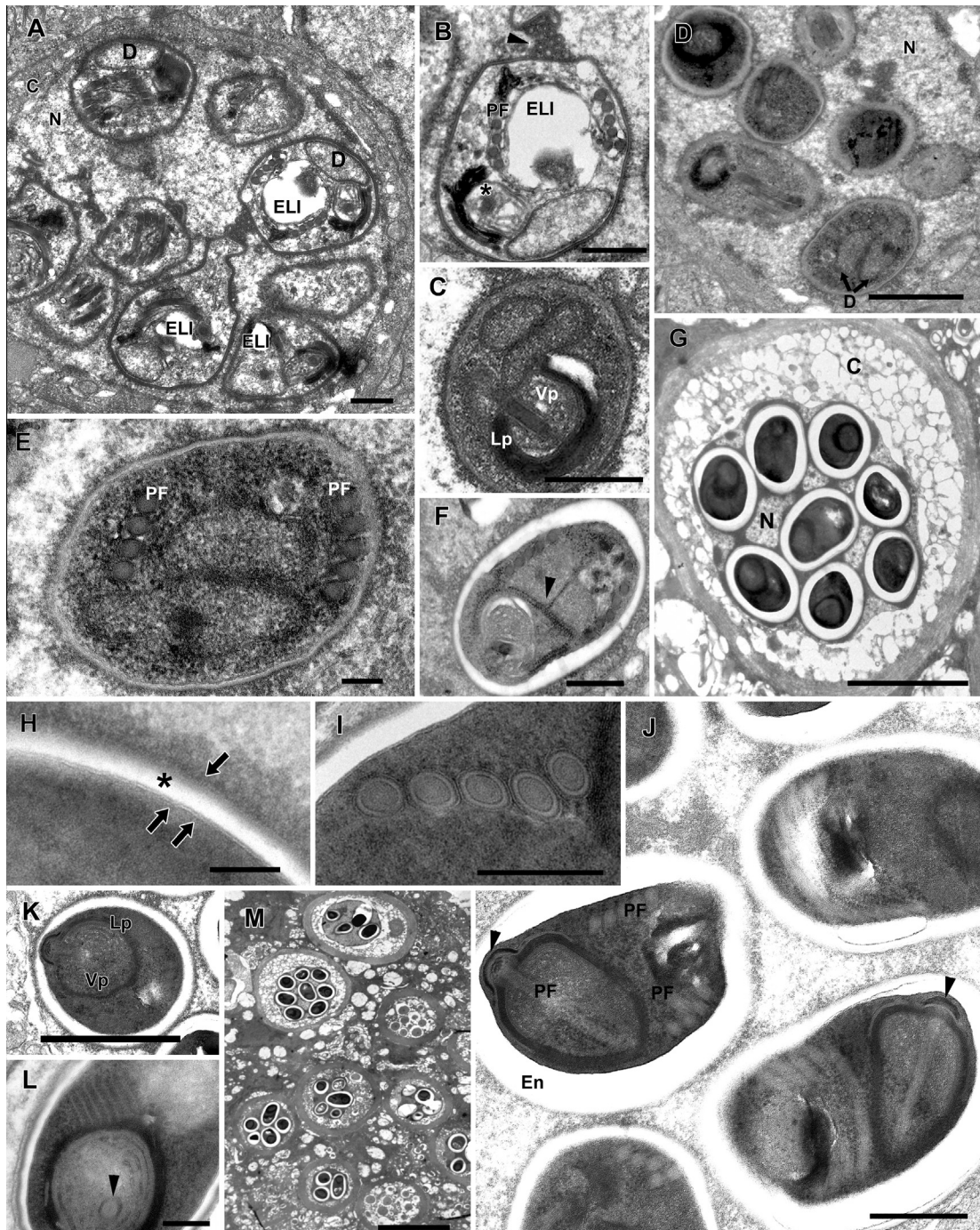


Fig. 4. Transmission electron micrographs showing the ultrastructure of intranuclear stages of *Enterospora nucleophila* in intestinal cells of *Sparus aurata*. (A) Early sporoblasts (nine are visible), immediately after plasmal division, in direct contact with the host nucleoplasm. Each sporoblast has a thickened plasmalemma surrounding the diplokaryon, the polar filament and the polaroplast. (B) Detail of one sporoblast in which the electron lucent inclusions is greatly enlarged and surrounded by the forming polar filament; the early polaroplast is visible (*). Some electron-dense disks are attached to the sporoblast surface (arrowhead). (C) A more advanced sporoblast. Note the presence of the outer lamellar and inner vesicular polaroplast surrounding the manubriod portion of the polar filament above the diplokaryon. (D) Numerous late sporoblasts in the host nucleoplasm. (E) Detail of one sporoblast showing the diplokaryon, transverse sections of the polar filament, abundant ribosomes and the commencement of the lucent endospore wall formation. (F) A spore with polyribosomes arranged in belts around the polaroplast (arrowhead); the diplokaryon and the thickened endospore are visible. (G) Nucleoplasm of a rodlet cell filled with spores which are covered with host heterochromatin. Note the vacuolisation of the host cytoplasm. (H) Detail of the exospore (one arrow), the endospore (*) and the plasmalemma (two arrows) of a mature spore. Notice the host chromatin closely attached to the exospore (one arrow). (I) Cross-section of five coils of the isofilar polar filament. (J) Mature spores containing the anchoring disks (arrowheads) and the portions of the five to six coils of the polar filament. (K) Detail of anterior spore structures, including the polaroplast in which the anchoring disk complex is attached to both the polar filament and the thinnest portion of the endospore. Note the elaborate polaroplast now filling at least half of the mature spore. (L) Detail of another spore in which the vesicular and lamellar polaroplast are visible surrounding the anterior (manubriod) portion (arrowhead) of the polar filament. (M) Low magnification view of a heavy infection of rodlet cells. Note the vacuolisation of the host cytoplasm. Scale bars: H = 100 nm; I, L = 200 nm; A, B, F, J = 500 nm; D, K = 1,000 nm; E, G = 2,000 nm; M = 5,000 nm, C = 1 μm. C, host cytoplasm; D, diplokaryotic nuclei; En, endospore; ER, endoplasmic reticulum; Lp, lamellar polaroplast; N, host nucleus; PF, polar filament; Vp, vesicular polaroplast.

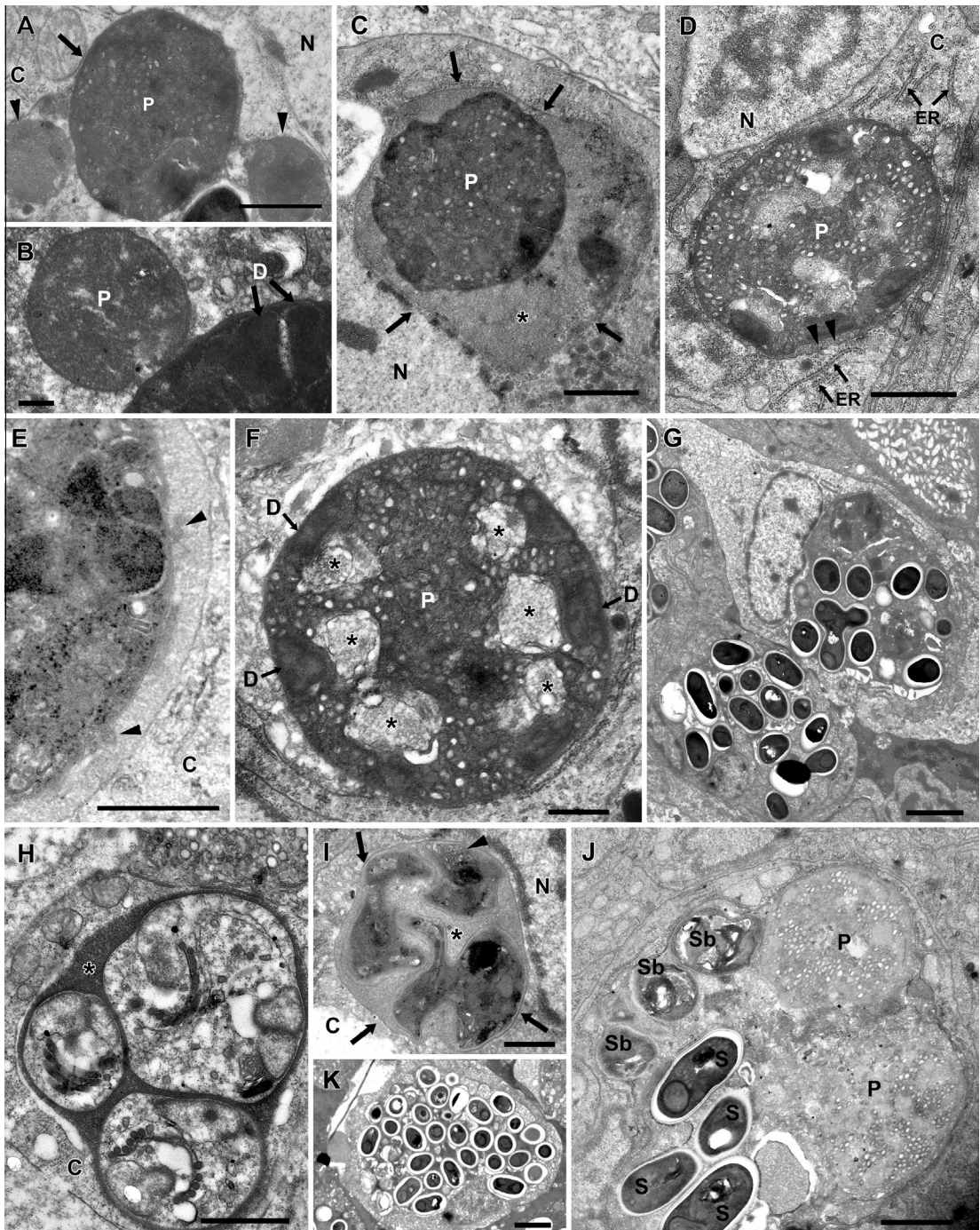


Fig. 5. Transmission electron micrographs showing the ultrastructure of the cytoplasmic infection of *Enterospora nucleophila* in intestinal cells of *Sparus aurata*. (A) The earliest stages observed are small merogonial plasmodia (arrowheads). Note the size difference with a more advanced plasmodium (arrow). (B) Large and small merogonial plasmodia; a well-defined plasmalemma is visible in the smaller one, the diplokarya are visible in the largest (arrows). (C) Plasmodium embedded in a dense matrix (*) and surrounded by an interfacial envelope (arrows) with nuclei arranged in diplokarya. Note the close association of the matrix with the host nucleus. (D) In some sections only a thin rim of the matrix is visible surrounding the plasmodium (arrowheads). Note the abundant host mitochondria and rough Endoplasmic Reticulum (arrows). (E) Detail of the interfacial envelope and the structures (arrowheads) observed within the matrix. (F) A more advanced plasmodium in which parasite diplokaryotic nuclei (arrows) are visible closely abutting the plasmalemma. Note the presence of abundant electron-dense disks and electron lucent inclusions (*) associated with each nuclear pair. (G) Mature spores and sporoblasts present in the cytoplasm of infected cells. Note the variation of the matrix appearance. (H) Early sporoblast formation after plasmodial division within a dense matrix (*). (I) Later sporoblast development in a less dense matrix (*); arrows indicate the interfacial envelope; arrowhead points to a polaroplast. (J) Asynchronous development is illustrated by the presence of two large plasmodia, three sporoblasts and numerous spores within a large parasitophorous vacuole. (K) Macrophage with numerous spores in its cytoplasm. Scale bars: B = 200 nm; D–F, J = 500 nm; H = 600 nm; C = 750 nm; A, G, I = 1,000 nm. C, host cytoplasm; D, diplokaryotic nuclei; ER, endoplasmic reticulum; N, host nucleus; P, plasmodium; S, spore; Sb, sporoblast.

was not consistently resolved. This instability mostly affected the branching of *E. cancri* relative to *En. bieneusi* and to the clade containing the GSBM and BTSM genotypes. The branching of an

uncharacterised *Nucleospora* sp. from eels (*Anguilla rostrata*) and an environmental genotype retrieved from pyrosequencing studies of marine anoxic water samples (uncultured stramenopile Gen-

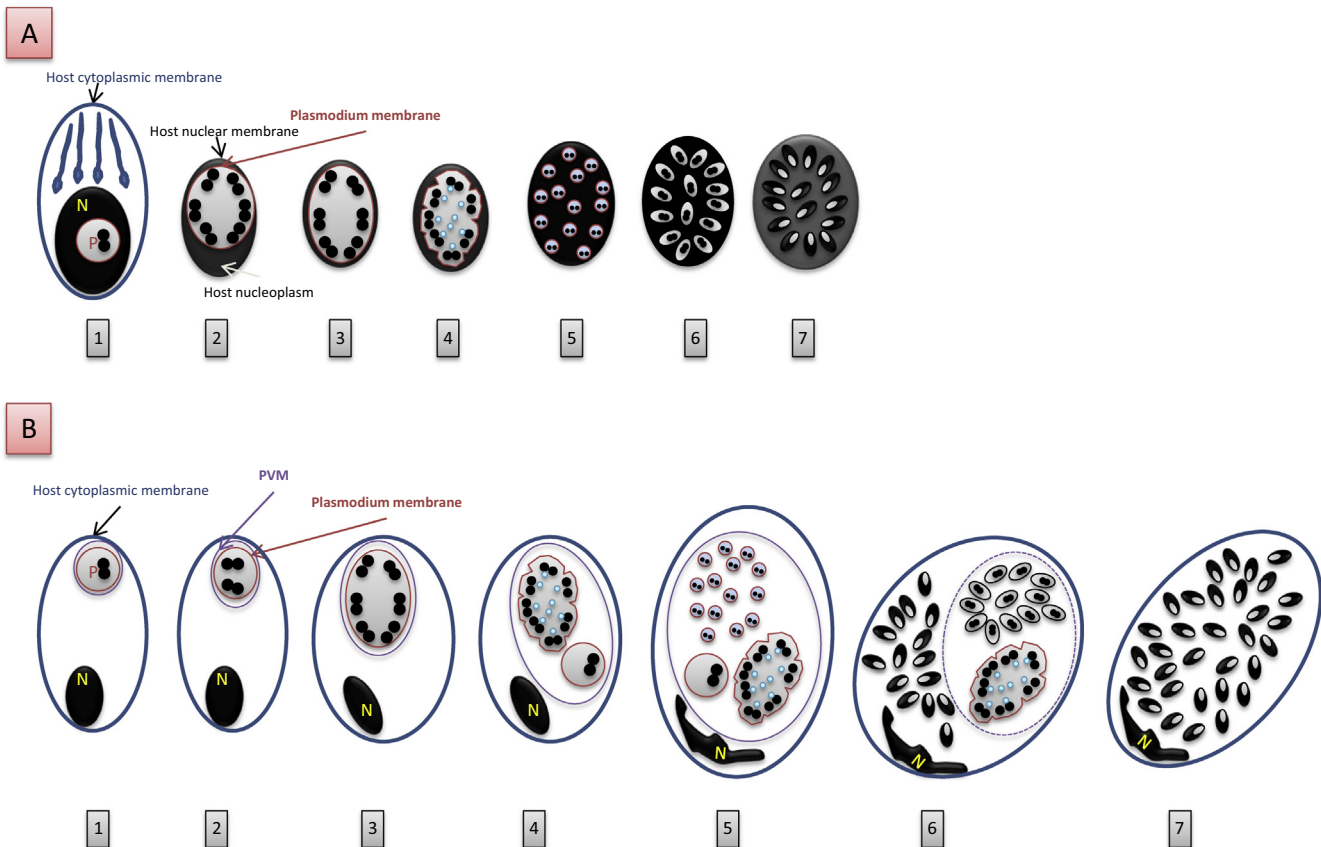


Fig. 6. Diagrammatic interpretation of the intranuclear (A) and cytoplasmic (B) stages of *Enterospora nucleophila*. (A) The infection starts in the host nucleus with an early binucleate meront (1), then merogonial plasmodium (2, 3) with a single plasmodial membrane developed free in the nucleoplasm; diplokarya are visible. The differentiation of the extrusion apparatus occurs before plasmotomy in the sporogonial plasmodium (4); sporoblasts appear and mature (5, 6) and finally spores are visible in the host nucleoplasm (7). (B) The infection starts with an early binucleate meront in the cytoplasm of the host cell surrounded by the membrane of the parasitophorous vacuole (1), which subsequently divides, producing a merogonial plasmodium (2, 3). The division and maturation process is asynchronous with different merogonial and sporogonial plasmodia at different stages (4–6). Finally multiple spores are found free in the host cytoplasm (7) without any interfacial envelopment. N, host nucleus; P, plasmodium; PVM, parasitophorous vacuole membrane.

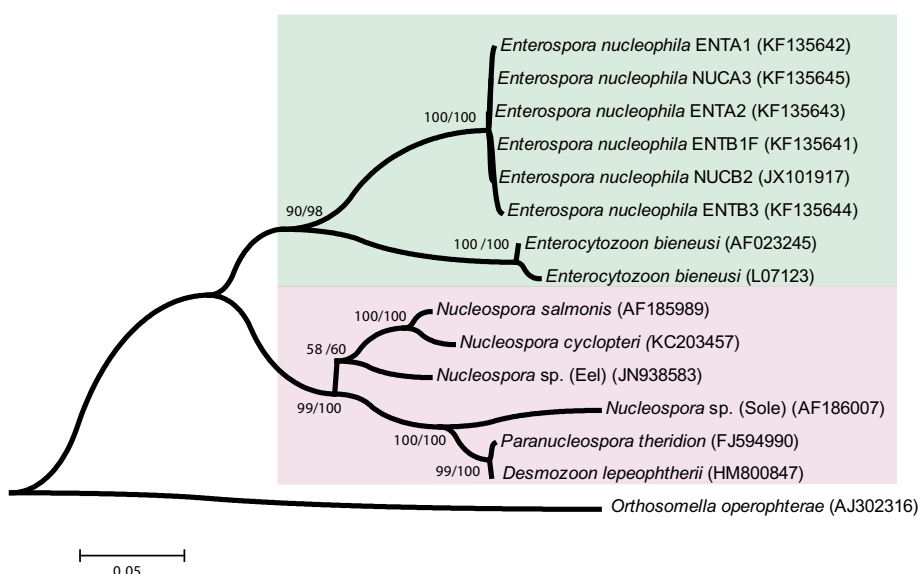


Fig. 7. ssrDNA cladogram of long (>1,000 bp) Enterocytozoonid sequences for which biological and genetic data are available, including the new *Enterospora nucleophila* genotypes. The topology was inferred using a dataset with 1,280 aligned sites, using maximum likelihood (ML) inference methods, and the tree with the highest log likelihood is shown (ML with a Tamura-Nei model and a discrete gamma distribution with invariant sites). Branch lengths are drawn to scale based on the number of nucleotide substitutions per site. Numbers at the nodes represent branching support by bootstrap values (500 resamplings of this dataset), and Bayesian posterior probabilities. *Orthosomella operophterae* was used as the outgroup. The main clades are shaded in different boxes.

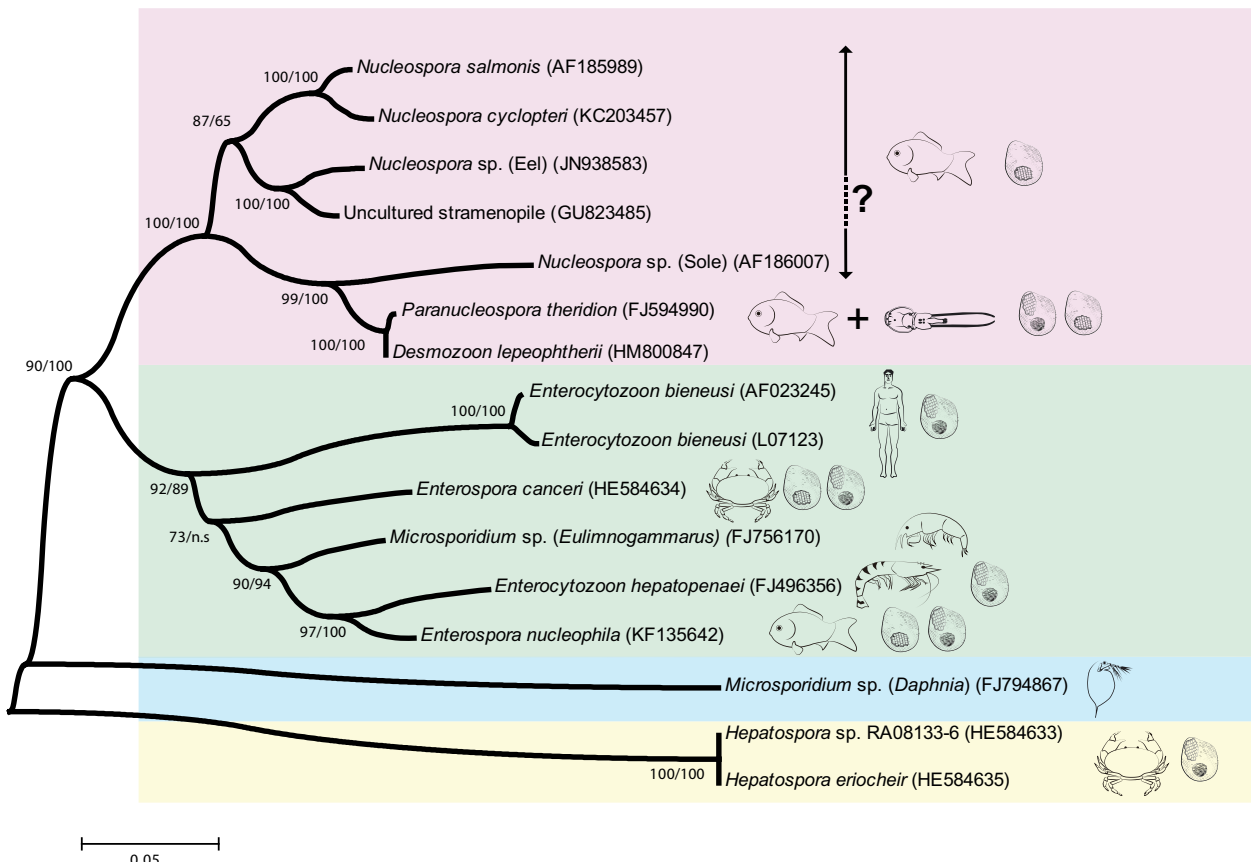


Fig. 8. Unrooted ssrDNA cladogram of the Enterocytozoonidae and related species including partial sequences of *Hepatospora* spp., *Enterospora cancri* and additional uncharacterised crustacean and environmental genotypes (*Microsporidium* spp.). The available biological information is also represented. The topology was inferred using a dataset with 1,280 aligned sites, using maximum likelihood inference methods and the tree with the highest log likelihood is shown (maximum likelihood with a General Time Reversible model with discrete gamma distribution). Branch lengths are drawn to scale based on the number of nucleotide substitutions per site. Numbers at the nodes represent branching support by bootstrap values (500 resamplings) and Bayesian posterior probabilities in consensus trees. *Hepatospora* spp. and *Microsporidium* sp. from *Daphnia* are resolved as independent clades from the other enterocytozoonid lineages and the branching of *Enterospora cancri* and *Nucleospora* spp. is unstable. The main clades are shaded in different boxes.

Bank Accession No. GU823485; Edgcomb et al., 2011), relative to other *Nucleospora* spp., was also unstable. Thus, grouping of *Enterospora* and the GSBM + BTSM to the exclusion of *En. bieneusi* was not reliably supported under some substitution models and particularly using stringent alignment sampling masks (Fig. 8 and data not shown). Specific analyses were carried out to address this issue, focusing only on the *Enterocytozoon* subclade. Under these conditions, moderate to high support for the clustering of GSBM with *E. cancri* as a sister group to *En. bieneusi* was obtained (Fig. 9).

3.4. Taxonomic summary

- Phylum: Microsporidia Balbiani, 1882.
- Class: Terresporidia Vossbrink and Debrunner-Vossbrinck, 2005.
- Order: Microsporida Balbiani, 1882.
- Family: Enterocytozoonidae Cali and Owen, 1990.
- Genus: *Enterospora* Stentiford, Bateman, Longshaw and Feist, 2007.
- Species: *Enterospora nucleophila* n. sp.
- Diagnosis of the species: ellipsoidal, diplokaryotic, fixed spores 1.67 × 1.05 µm in size, with 5–6 isofilar polar filament coils in a single row. Merogonial and sporogonial plasmodia with diplokarya. Polysporous development in the nucleus of enterocytes and rodlet cells without interfacial envelope and in the cytoplasm of enterocytes and phagocytes with interfacial

envelope. Up to 16 spores develop in the host cell nuclei as a result of a single infection event. More than 40 spores can be present in the cytoplasm as a result of several asynchronous developmental cycles, all within a single interfacial envelope.

- Type host: *Sparus aurata* (Teleostei: Sparidae).
- Site of infection: primarily intestine, rarely in the stomach.
- Prevalence: variable, up to 80% in some stocks.
- Type locality: aquaculture earth ponds at southwest Spain (Atlantic coast).
- Etymology: the species is named after its preferential location in the host cell nucleus.
- Type material deposited: histological resin sections with infected material have been deposited in the Museo Nacional de Ciencias Naturales (MNCN-CSIC), Madrid (Spain) with numbers MNCN 36.02/5 for the holotype and MNCN 36.02/6 for the paratype. Gene sequence: Sequences comprising almost the complete ssrDNA (1278 bp) of *E. nucleophila* isolates have been deposited in GenBank database under Accession numbers JX101917 and from KF135641 to KF135645.
- Amended diagnosis of the family Enterocytozoonidae: the microsporidians included in this family are unified by a ssrDNA-based molecular phylogeny and by the nature of polar filament formation. They constitute a monophyletic clade rooted within the clade IV or Class Terresporidia as defined by Vossbrinck and Debrunner-Vossbrinck (2005). The only unifying morphological characters are the precocious polar filament

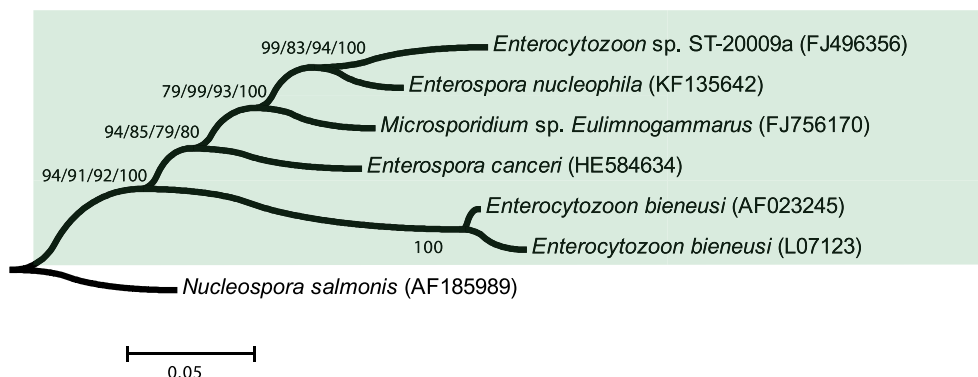


Fig. 9. ssrDNA cladogram of the Enterocytozoonidae rooted with *Nucleospora salmonis* and focused on the relationships in the *Enterocytozoon/Enterospora* subclade. The topology shown was inferred using a dataset with 1,280 aligned sites, using maximum likelihood inference methods and the tree with the highest log likelihood is shown (maximum likelihood with a Hasegawa-Kishino-Yano model and a discrete gamma distribution with invariant sites). Numbers at the nodes represent branching support values (after 500 resamplings of this dataset), or Bayesian posterior probabilities, in consensus trees, as calculated by: (i) distance methods; (ii) maximum parsimony; (iii) maximum likelihood; and (iv) Bayesian analysis.

formation and the means by which they develop (the polar filament complexes organise around the nuclei before the sporogonic plasmodium begins cell division into sporoblasts). Other characters such as nucleation (isolated or in diplokaryotic arrangement), location within the host cell nucleus or cytoplasm, and presence or absence of interfacial envelopes, should be considered, however, as secondary characters of the genera or species in the family. It should also be noted that this family occurs in a wide range of hosts and environments, including aquatic crustaceans and fish and terrestrial mammals including humans.

4. Discussion

Enterocytozoon bieneusi was initially described from a human intestinal infection (Desportes et al., 1985). This parasite was later found to have unique developmental features which were incorporated into the new family Enterocytozoonidae (Cali and Owen, 1990). *Enterocytozoon bieneusi* is now considered the most prevalent human microsporidian (Matos et al., 2012) and it has been reported in several other mammals and birds (Matos et al., 2004; Lobo et al., 2006). Additionally, fish and invertebrates including crabs have been reported to harbour microsporidians belonging to this family, resulting in the proposal of five genera and multiple species assigned (Modin, 1981; Hedrick et al., 1991; Lom and Dyková, 2002; Stentiford et al., 2007, 2011; Freeman and Sommerville, 2009; Nylund et al., 2010; Freeman et al., 2013). In addition, recent environmental and ecological studies involving planktonic crustaceans have generated DNA sequence data that, although unassigned to well-characterised microsporidian phenotypes, cluster within the Enterocytozoonidae in ssrDNA-based phylogenies. The relevant features of the main known members of this family are compared in Table 2.

The microsporidian described in the current study shares with the family Enterocytozoonidae the early appearance of ELIs and EDDs as the polar filament precursors and the assembly of the components of the extrusion apparatus before division of the plasmodium to form sporoblasts. Additionally, the molecular analysis of ssrDNA roots the species firmly within the family Enterocytozoonidae. According to a ssrDNA-based molecular phylogeny of known species of this family, there are two well-supported enterocytozoonid subclades represented by: (i) nuclear infecting/developing microsporidia from fish and crustaceans (*Nucleospora* and *Paranucleospora/Desmozoon*); (ii) *Enterocytozoon*, *Enterospora* and the species studied in this work. To these enterocytozoonid lineages, a third one containing *Hepatospora* spp. sequences (and even

a fourth one exemplified by the genotype MIC-2 from *Daphnia*) appear related, although the sequence data are too limited to infer solid relationships between them; currently, these taxa appear as sisters to "true" Enterocytozoonidae (*Nucleospora*, *Paranucleospora*, *Enterospora* and *Enterocytozoon*). Their assignment to Enterocytozoonidae is conservative, responding to the fact that unclear higher level taxonomy of the phylum prevents erection of novel suprageneric taxa (Vossbrinck and Debrunner-Vossbrinck, 2005; Stentiford et al., 2011). It must be stressed that Microsporidia are characterised by an extreme reduction of genome size and, consequently, shortened ssrDNAs. Thus, inference of higher level relationships between divergent lineages using incomplete sequence (e.g., those from *Hepatospora* spp. or from environmental studies) results in a low phylogenetic signal-to-noise ratio and poor resolution of these clades.

Within the Enterocytozoonidae, the novel species from gilthead sea bream appeared very closely related to *En. hepatopenaei* (89.6% pairwise identity along the common ssrDNA segment). The genotype BVER2 from the amphipod *Eu. verrucosus* also clustered with these two species in a well-supported clade, which was consistently resolved as a sister clade to *En. bieneusi*. *Enterospora canceri* rooted in this same branch of the tree but its position suffered some instability. Under most inference methods and substitution models, *E. canceri* was resolved as closer to the aquatic subclade than to *En. bieneusi*, but the support for this arrangement was only moderate, probably due in part to the limited phylogenetic signal provided by a shorter *E. canceri* sequence. According to these results, there is strong support for the grouping of the gilthead sea bream microsporidian, the species from black tiger shrimp, and the genotype from the amphipod *Eu. verrucosus*, as congeneric species. A sister relationship of this clade with *E. canceri* also seems well supported in most analyses. Since previous studies have proposed the assignment of the shrimp species *En. hepatopenaei* to *Enterospora*, rather than to *Enterocytozoon* (Stentiford et al., 2011), we propose the placement of the GSBM in this same genus and we name it *Enterospora nucleophila*. This arrangement resolves a monophyletic genus *Enterospora* with a sister relationship to *Enterocytozoon*, all of them constituting an independent enterocytozoonid lineage that branches off *Nucleospora*, *Paranucleospora*/ *Desmozoon* and other fish and crustacean species. This genus would also include the yet undescribed *Microsporidium* sp. genotype from the amphipod *Eu. verrucosus* (GenBank Accession No. FJ756170). It must be stressed that we consider this assignment conservative due to the somewhat unclear relationship of *E. nucleophila* and *En. hepatopenaei* with *E. canceri*. More genetic data for *E. canceri* and other related crab genotypes could provide a better

Table 2

Biological and molecular data of the main microsporidians related to the family Enterocytozoonidae.

Species	Dipk ^a	Location	I.E. N	S.S. C	No. of spores/ group	Spore size (μm)	No. of coils	Bin. sp.	Host group	Cell type	Xen	ssrDNA (GB Ref.) ^e	ssrDNA length (bp)		
<i>Enterocytozoon bieneusi</i>	x	x	x	✓	x	x	24	1.5 × 0.9	5–6	x	M, B	ENT	x	AF023245 L07123	1,284 1,248
<i>Enterocytozoon hepatopenaei</i>	x	x	x	✓	✓	na	>20	1.1 × 0.7	5–6	x	Cr	EPI	x	FJ496356	848 ^g
<i>Hepatospora eriocheir</i>	x	x	✓	✓	✓	✓	>40	1.8 × 0.9	7–8	x	Cr	HEP	x	HE584635	957
<i>Microsporidium rhabdophilia</i>	na	✓	x	na	na	na	>16	1.05 × 2.9	na	na	Fish	RC	x	na	na
<i>Nucleospora cyclopteri</i>	na	✓	x	na	na	1–14	3.12 × 1.3	na	na	Fish	LYMPH	x	KC203457	1,182	
<i>Nucleospora salmonis</i>	x	✓	x	x	na	2–20	2 × 1	8–12	x	Fish	BC	x	AF185989	1,250	
<i>Nucleospora secunda</i>	x	✓	x	x	na	7–18	1.6 × 0.8	4–5	x	Fish	ENT	x	na	na	
<i>Nucleospora</i> sp. (Eel)	na	✓	x	na	na	na	na	na	na	Fish	na	x	JN938583	1,191	
<i>Nucleospora</i> sp. (Sole)	na	✓	x	na	na	na	na	na	na	Fish	na	x	AF186007	1,284	
<i>Desmozoon lepeophtherii</i> ^c (syn. <i>Paranucleospora theridion</i>)	✓	✓ ^b	✓	x	na	2–4	1.05/ 2.55 × 2.05	1–2/5– 6	✓	Fish	EDC, PHY	x	HM800847	1,283	
<i>Enterospora cancri</i>	x	✓	✓ ^d	x	x	>200	1.3 × 0.7	4–5	x	Cr	DMC	✓	FJ594990	1,286	
<i>Enterospora nucleophila</i>	✓	✓	✓	✓	✓/x	16/>40	1.67 × 1.05	5–6	✓	Fish	HEP ENT, RC	x	HE584634 JX101917	816 1,298	
<i>Microsporidium</i> sp._MIC-2	na	na	na	na	na	na	na	na	na	Cr	na	na	JF94867	1,186	
<i>Microsporidium</i> sp. VBER2	na	na	na	na	na	na	na	na	na	Cr	na	na	FJ756170	719	
Uncultured stramenopile	na	na	na	na	na	na	na	na	na	na	na	na ^f	na	GU823485	1,026

na, not available; x, not observed; ✓, observed; I.E., interfacial envelope; S.S., synchronous sporogenesis; Bin. Sp., binuclear spore; N, nuclear; C, cytoplasmic; ENT, enterocytes; EPI, epithelial cells; HEP, hepatopancreocytes; LYMPH, lymphocytic cells; RC, rodlet cells; BC, blood cells; EDC, epidermal cells; PHY, phagocytes; DMC, desmocytes; Cr, crustacean; M, mammals; B, birds; Xen, Xenoma-forming species; GB Ref, GenBank accession number.

^a Diplokaryon observed in at least one stage of development.

^b Only in fish stages.

^c Spore data in the fish cycle correspond to two types of spores.

^d Occasionally, also in cells with infected nuclei.

^e When multiple genotypes are available, those used in this work are listed.

^f Retrieved from environmental, filtered marine water samples (microplankton).

^g The ends of this sequence were found unreliable and edited: aligned segment was 810 bp.

insight into this relationship and might reveal *E. nucleophila* and *En. hepatopenaei* as a separate lineage deserving independent generic status.

According to biological, morphological and ultrastructural criteria, *E. nucleophila* does not fit any of the genera described thus far in the family Enterocytozoonidae. This is not surprising given the paucity of available morphometric diagnostic characters and the heterogeneity in hosts, environments and life cycles that can be found in this family. *Enterospora nucleophila* exhibits both intranuclear and cytoplasmic development. There are other members of the Enterocytozoonidae that can develop in both cellular niches, found in different enterocytozoonid subclades: *P. theridion* (Nylund et al., 2010) and *E. cancer* (Stentiford et al., 2007). The latter seems able to develop spores in both locations of a single cell in advanced infections, whereas in *E. nucleophila* no host cells were found infected simultaneously at both sites. Furthermore, despite being closely related, *En. hepatopenaei* and *En. bieneusi* do not have any known intranuclear stages. This variability clearly illustrates the limited usefulness of even what was considered a key developmental feature to classify species in this family. The intranuclear spores of *E. nucleophila* are interpreted to result from a single cell invasion event, whereas the cytoplasmic ones seem to correspond to several asynchronous episodes of sporogenesis. Although cytoplasmatic spores are clearly more numerous than the intranuclear ones, as in *P. theridion*, they are morphologically identical. Besides the morphology, several lines of evidence prompt us to consider that the organism detected in both cytoplasmatic and intranuclear sites is a single species. Firstly, infections in both sites were present frequently (e.g., 42.9% of the infected fish in 2011 samplings) and the dominance of intranuclear stages was clearly associated with

early infections. This lead us to interpret a sequence course of infection starting in the nuclei of RCs at the epithelial layer and a subsequent dispersion to other cell types at cytoplasmatic niches, most likely via phagocytosis by enterocytes and macrophages. Secondly, we found only minor genetic variation within and between clones from two samples selected by the predominance of either type of infection. Finally, such development at both cellular niches occurs in other species of the family (Stentiford et al., 2007; Nylund et al., 2010). Concomitant infections by different enterocytozoonid species invading both cellular sites simultaneously are yet to be described and in our case they seem highly unlikely, even though we cannot completely rule out this possibility.

Concerning other morphological features of the Enterocytozonidae, no interfacial envelope has been found in any of the intranuclear species (spores are dispersed freely in the host nucleoplasm) studied to date, whereas its presence in cytoplasmic stages seems variable. In *En. hepatopenaei*, some plasmodia were found within a vacuole while others were not (Tourtip et al., 2009). In *Hepatospora*, a sporophorous vacuole was observed (Stentiford et al., 2011) and in the cytoplasmic stages of *D. lepeophtherii*, a secretion from the exospore formed a fragile interfacial envelope that created a void surrounding the spore (Freeman and Sommerville, 2009). The envelope surrounding the cytoplasmic stages of *E. nucleophila* was interpreted as the membrane of a parasitophorous vesicle or vacuole, since it was visible even around non-sporogonic plasmodia. According to Nilsen et al. (1998), the sporophorous vesicle could have developed several times during microsporidian evolution. It is tempting to speculate that naked intranuclear stages respond to parasites sporoplasms being injected directly into the host nucleus, where they are safe from host attack,

whereas in the cytoplasm of the host cell they can eventually present a parasitophorous vacuole membrane (PVM), depending on the strategy used to breach it (Franzen, 2005). It is also remarkable that most cytoplasmic stages of *E. nucleophila* were found in macrophages, since phagocytosis is the most likely mode of entrance; or in enterocytes, in which intracellular translocation of bacteria by endocytosis and encapsulation by a membrane vacuole have been described in fish (Ringø et al., 2010).

The diplokaryotic nuclei arrangement found in several stages of *E. nucleophila* seem to be shared only with the fish stages of *P. theridion*/ *D. lepeophtherii* (Nylund et al., 2010; Freeman and Sommerville, 2009) among its closest relatives. By contrast, *En. bieneusi* does not have diplokarya in any stage of development (Cali and Owen, 1990) and this detail was not provided for the genus *Enterospora*, as only an early plasmodial stage with ‘paired nuclei’ was noted (Stentiford and Bateman, 2007). The occurrence of diplokarya in microsporidian development was considered an important character in classification (reviewed by Sprague et al., 1992), but it is currently considered a plesiomorphic trait with low taxonomic weight (Vossbrinck and Debrunner-Vossbrinck, 2005).

The morphology of the *E. nucleophila* spore does not have differential value compared with other related microsporidians and is not crucial for the erection of this new species. The number of polar tube turns is similar to that of *En. bieneusi* and *En. hepatopenaei* (five to six coils). In contrast, *N. salmonis* possesses eight to twelve and *P. theridion* intranuclear spores have a very short polar filament (one to two turns). The spore size of *E. nucleophila* is also within the range of other species of this family (Table 2).

The ultrastructural features of the merogonial and sporogonial plasmodia of *E. nucleophila* resemble those of *En. bieneusi* and *N. salmonis*. The EDDs of *E. nucleophila* seem much more abundant and the ELIs also appear more abundant in later plasmodial development. While they have been interpreted as precursors of the polar tube and the anterior attachment complex, they could possibly also participate in spore wall formation, since they were observed attached to the wall of the sporoblasts. Based on previous reports and demonstration of Golgi in all stages of microsporidian development (Takvorian et al., 2013), it is tempting to suggest that a form of Golgi is also present in the Enterocytozoonidae, especially in the formation of the ELIs.

From an ecological and evolutionary perspective, the range of hosts and development found in the Enterocytozoonidae is strikingly diverse and further illustrates the biological plasticity of this family. Although the biological information associated with some species descriptions is rather limited, it seems evident from the phylogenetic analysis that lineages in this group have switched from cytoplasmatic to intranuclear niches on several occasions independently, and present both alternative development (sometimes simultaneously, e.g. in *E. nucleophila*) in relatively closely related species. In addition, the adoption of hosts appears rather promiscuous, including vertebrates and invertebrates from aquatic habitats but also terrestrial vertebrates in *En. bieneusi*. This suggests trophic-related host-transmission mechanisms, as have been demonstrated in *P. theridion* (between vertebrate and invertebrate hosts) (Nylund et al., 2010). While rooting in a lineage of crustacean parasites, some of which can also develop in fish as alternate hosts, only vertebrate hosts are known for *E. nucleophila* and *En. bieneusi*. Thus, it seems likely that invertebrate hosts could be involved in the transmission of *E. nucleophila* to gilthead sea bream, as has been suggested for the crab and shrimp species, *E. cancerri* and *En. hepatopenaei* (Stentiford et al., 2011, 2013). This observation also contributes to the long-standing debate on the existence of unknown vectors for human and animal infections with *En. bieneusi*. In the case of *E. nucleophila*, the existence of such vector(s) would explain the outbreaks in gilthead sea bream in ponds and net cages, where diverse planktonic crustaceans are ubiquitous. It

also seems noteworthy to point out that live crustaceans (i.e. *Artemia* spp.) are routinely used as live prey in the early stages of marine fish rearing. In fact, previous studies with the microsporidian *Glugea stephani* clearly demonstrated the role of this crustacean as a vector in experimental infections of winter flounder, *Pseudopleuronectes americanus*, after placing *Artemia* in a spore-rich environment for a few hours (Cali et al., 1986). Even though clinical signs of infection by *E. nucleophila* in gilthead sea bream are usually observed in growing fish, an earlier acquisition of the parasite through live prey cannot yet be ruled out.

Host cell types and host tissues infected by members of the Enterocytozoonidae are quite variable, although certain affinities can be discerned. The targeting of epithelial cells shown by *E. nucleophila* is shared with *Enterospora* spp. infecting crustaceans (Stentiford et al., 2007; Tourtip et al., 2009) and by species of *Enterocytozoon*, with *En. bieneusi* predominantly infecting the enterocytes of the human duodenum and ileum (Desportes et al., 1985). Other locations in the hosts are listed in Table 2.

Intranuclear stages of *E. nucleophila* were mainly present in RCs, which were extraordinarily numerous and present even in the intestinal submucosa. Two other intranuclear microsporidia have been described in RCs: *Microsporidium rhabdophilia* and *N. salmonis*, both infecting salmonids. RCs are exclusive to fish and represent a cell type closely linked to piscine inflammatory cells (Reite, 2005). Many studies consistently report an association between RC proliferation/hyperplasia and the presence of a variety of parasites (reviewed by Manera and Dezfuli, 2004), and in particular in gilthead sea bream (Palenzuela et al., 1999; Dezfuli et al., 2011). However, the density of infected RCs found in our study is clearly higher than the findings depicted in such cases and results in a very conspicuous hypercellularity in infected intestines. Similarly, *N. salmonis* induces an unusual proliferation in lymphopoietic cells (Wongtavatchai et al., 1995). In gilthead sea bream, RCs appear to be almost the only cell type involved in the response to the infection while restricted to the epithelium, since in most cases no cellular proliferation or migration of lymphocytes was observed and granulocytes were rather scarce. Only when *E. nucleophila* spread to other intestinal sites were macrophages, MMC and granulocytes abundant in the submucosa. Macrophages seem to participate in the resistance and clearing of fish microsporidian spores but some parasites seem capable of blocking the intracellular killing mechanisms of phagocytes (see Rodríguez-Tovar et al., 2011), thus avoiding their destruction by immune cells. In fact, it has been suggested that *P. theridion*-infected macrophages could be responsible for propagating the parasite within the host (Sveen et al., 2012). In the current study, macrophages appeared to perform both roles, since effete spores were observed within macrophages in fish with old infections but infected macrophages also appeared to have migrated from the epithelium to the submucosa, where they can spread to other sites. The infected cells observed in blood vessels at the submucosa and in muscle or liver provide further support for this route of propagation within the host.

External signs of disease in crustaceans caused by Enterocytozoonidae have not been stressed in most cases (Stentiford et al., 2007, 2011; Stentiford and Bateman, 2007; Tourtip et al., 2009) and the significance of these infections as drivers of mortality in wild crustaceans has not been assessed. However, severe lesions caused by *E. cancerri* were reported in *Cancer pagurus* (Stentiford et al., 2007) and *En. hepatopenaei* has been associated with the so-called “Monodon slow growth syndrome” (Chayaburakul et al., 2004). By contrast, several fish-infesting species provoke mortality in aquaculture settings of salmonids (Morrison et al., 1990; Chilmomczyk et al., 1991; Nylund et al., 2011; Sveen et al., 2012) and other species (Mullins et al., 1994; Nilsen et al., 1995). The pathological effect of *E. nucleophila* in gilthead sea bream and the associated mortality in different types of facilities in distant sites over

several years leads us to consider this microsporidian parasite a potential threat for growing stocks. In any case, the precise role of this parasite in causing disease has to be confirmed by challenge experiments and further epidemiological studies. It has been suggested that related species, such as *En. hepatopenaei*, might be opportunistic in nature and exploit a weakened host immune status (Tourtip et al., 2009). In gilthead sea bream, this is an interesting possibility to explore since outbreaks appear to occur more frequently in colder areas and by the end of winter, when this fish suffers a weakened immune status and high incidence of a multi-factorial "Winter Syndrome" (Tort et al., 1998). The host and the geographic range of this new microsporidian also needs to be established, since other members of this family such as *N. salmonis* seem to be ubiquitous in the waterways inhabited by many different salmonids worldwide (El Alaoui et al., 2006). Due to the small size and the cryptic nature of *E. nucleophila*, and the possibility of confounding some clinical signs with those of enteromyxosis (Sitjà-Bobadilla and Palenzuela, 2012), infections by this intranuclear microsporidian can be easily overlooked and they could be more prevalent than initially found in this study. Continued research efforts and the use of molecular diagnostic tools should contribute to clarifying the true pathogenic potential of *E. nucleophila* for the aquaculture industry.

Acknowledgments

This work was funded through CSIC (Spain), Internal Research Programmes (Intramural projects refs. 200430E560 and 201330 E025), and additional research Grants from the regional Government (Generalitat Valenciana refs. PROMETEO 2010/006 and ISIC/003). Collaboration with fish health consultants G. Albinyana (Immuno-vet), E. Planas (BioMar) and C. Zarza (Skretting), and with fish farming companies is gratefully acknowledged. We thank Dr. Mark Freeman (Institute of Biological Sciences, University of Malaya (Malaysia)) and Dr. Grant Stentiford (CEFAS, UK) for their comments and scientific exchange during this study. We also thank J. Monfort and L. Rodríguez for histological processing and the staff at the Servei Central de Suport a la Investigació Experimental (SCSIE) of the University of Valencia (Spain) and at the Rutgers-Newark Electron Microscopy facility (USA), for technical support in TEM processing. Phylogenetic artwork was prepared by I. Castell (i.castell@hotmail.com).

References

- Abdel-Ghaffar, F., Bashtar, A.R., Mehlhorn, H., Al-Rasheid, K., Morsy, K., 2011. Microsporidian parasites: a danger facing marine fishes of the Red Sea. *Parasitol. Res.* 108, 219–225.
- Abela, M., Brinch-Iversen, J., Tanti, J., Le Breton, A., 1996. Occurrence of a new histozoic microsporidian (Protozoa, Microspora) in cultured gilt head sea bream *Sparus aurata* L. *Bull. Eur. Assoc. Fish Pathol.* 16, 196–199.
- Altschul, S.F., Gish, W., Miller, W., Myers, E.W., Lipman, D.J., 1990. Basic local alignment search tool. *J. Mol. Biol.* 215, 403–410.
- Athanassopoulou, F., 1998. A case report of *Pleistophora* sp. infection in cultured sea bream (*Sparus aurata* L.) in Greece. *Bull. Eur. Assoc. Fish Pathol.* 18, 19–21.
- Cali, A., Owen, R.L., 1990. Intracellular development of *Enterocytozoon*, a unique microsporidian found in the intestine of AIDS patients. *J. Protozool.* 37, 145–155.
- Cali, A., Takvorian, P.M., Ziskowski, J.J., Sawyer, T.K., 1986. Experimental infection of American winter flounder (*Pseudopleuronectes americanus*) with *Glugea stephani* (Microsporidia). *J. Fish Biol.* 28, 199–206.
- Chayaburakul, K., Nash, G., Pratnapipat, P., Sriurairatana, S., Withyachumnarnkul, B., 2004. Multiple pathogens found in growth-retarded black tiger shrimp *Penaeus monodon* cultivated in Thailand. *Dis. Aquat. Org.* 60, 89–96.
- Chilmonczyk, S., Cox, W.T., Hedrick, R.P., 1991. *Enterocytozoon salmonis* n. sp. – an intranuclear microsporidium from salmonid fish. *J. Protozool.* 38, 264–269.
- Desportes, I., Charpentier, Y.L., Galian, A., Bernard, F., Cochand-Priollet, B., Lavergne, A., Ravisse, P., Modigliani, R., 1985. Occurrence of a new Microsporidian: *Enterocytozoon bieneusi* n. g. n. sp., in the enterocytes of a human patient with AIDS1. *J. Eukaryot. Microbiol.* 32, 250–254.
- Dezfuli, B.S., Castaldelli, G., Bo, T., Lorenzoni, M., Giari, L., 2011. Intestinal immune response of *Silurus glanis* and *Barbus barbus* naturally infected with *Pomphorhynchus laevis* (Acanthocephala). *Parasite Immunol.* 33, 116–123.
- Didier, E.S., Weiss, L.M., 2011. Microsporidiosis: not just in AIDS patients. *Curr. Opin. Infect. Dis.* 24, 490–495.
- Edgcomb, V., Orsi, W., Bunge, J., Jeon, S., Christen, R., Leslin, C., Holder, M., Taylor, G.T., Suarez, P., Varela, R., Epstein, S., 2011. Protistian microbial observatory in the Cariaco Basin, Caribbean. I. Pyrosequencing vs Sanger insights into species richness. *ISME J.* 5, 1344–1356.
- El Alaoui, H., Gresoviac, S.J., Vivares, C.P., 2006. Occurrence of the microsporidian parasite *Nucleospora salmonis* in four species of salmonids from the Massif Central of France. *Folia Parasitol.* 53, 37–43.
- Faye, N., Toguebaye, B.S., Bouix, G., 1990. Ultrastructure and development of *Pleistophora senegalensis* sp. nov. (Protozoa, Microspora) from the gilt-head sea bream, *Sparus aurata* L. (Teleost, Sparidae) from the coast of Senegal. *J. Fish Dis.* 13, 179–192.
- Franzen, C., 2005. How do microsporidia invade cells? *Folia Parasitol.* 52, 36–40.
- Freeman, M.A., Bell, A.S., Sommerville, C., 2003. A hyperparasitic microsporidian infecting the salmon louse, *Lepeophtheirus salmonis*: an rDNA-based molecular phylogenetic study. *J. Fish Dis.* 26, 667–676.
- Freeman, M.A., Sommerville, C., 2009. *Desmozoon lepeophtherii* n. gen., n. sp. (Microsporidia: Enterocytozoonidae) infecting the salmon louse *Lepeophtheirus salmonis* (Copepoda: Caligidae). *Parasite Vectors* 2, 58.
- Freeman, M.A., Sommerville, C., 2011. Original observations of *Desmozoon lepeophtherii*, a microsporidian hyperparasite infecting the salmon louse *Lepeophtheirus salmonis*, and its subsequent detection by other researchers. *Parasite Vectors* 4, 231.
- Freeman, M.A., Kasper, J.M., Kristmundsson, A., 2013. *Nucleospora cyclopteri* n. sp., an intranuclear microsporidian infecting wild lumpfish, *Cyclopterus lumpus* L., in Icelandic waters. *Parasite Vectors* 6, 49.
- Gill, E.E., Fast, N.M., 2006. Assessing the microsporidia-fungi relationship: combined phylogenetic analysis of eight genes. *Gene* 375, 103–109.
- Ghosh, K., Weiss, L.M., 2009. Molecular diagnostic tests for microsporidia. *Interdiscip. Perspect. Infect. Dis.*, 926521.
- Gresoviac, S.J., Baxa, D.V., Vivares, C.P., Hedrick, R.P., 2007. Detection of the intranuclear microsporidium *Nucleospora salmonis* in naturally and experimentally exposed Chinook salmon *Oncorhynchus tshawytscha* by in situ hybridization. *Parasitol. Res.* 101, 1257–1264.
- Griebel, T., Brinkmeyer, M., Böcker, S., 2008. EPoS: a modular software framework for phylogenetic analysis. *Bioinformatics* 24, 2399–2400.
- Hedrick, R.P., Groff, J.M., Baxa, D.V., 1991. Experimental infections with *Enterocytozoon salmonis* Chilmonczyk, Cox, Hedrick (Microspora): an intranuclear microsporidium from chinook salmon *Oncorhynchus tshawytscha*. *Dis. Aquat. Org.* 10, 103–108.
- Huelsenbeck, J.P., Ronquist, F., 2001. MRBAYES: Bayesian inference of phylogenetic trees. *Bioinformatics* 17, 754–755.
- Lee, S.C., Corradi, N., Byrnes, E.J., Torres-Martínez, S., Dietrich, F.S., Keeling, P.J., Heitman, J., 2008. Microsporidia evolved from ancestral sexual fungi. *Curr. Biol.* 18, 1675–1679.
- Lobo, M.L., Xiao, L., Cama, V., Magalhaes, N., Antunes, F., Matos, O., 2006. Identification of potentially human-pathogenic *Enterocytozoon bieneusi* genotypes in various birds. *Appl. Environ. Microbiol.* 72, 7380–7382.
- Lom, J., 2002. A catalogue of described genera and species of microsporidians parasitic in fish. *Syst. Parasitol.* 53, 81–99.
- Lom, J., Dyková, I., 2002. Ultrastructure of *Nucleospora secunda* n. sp (Microsporidia), parasite of enterocytes of *Nothobranchius rubripinnis*. *Eur. J. Protistol.* 38, 19–27.
- Ludwig, W., Strunk, O., Westram, R., Richter, L., Meier, H., Yadhukumar, Buchner, A., Lai, T., Steppi, S., Jobb, G., Forster, W., Brettske, I., Gerber, S., Ginhart, A.W., Gross, O., Grumann, S., Hermann, S., Jost, R., Konig, A., Liss, T., Lussmann, R., May, M., Nonhoff, B., Reichel, B., Streblow, R., Stamatakis, A., Stuckmann, N., Vilbig, A., Lenke, M., Ludwig, T., Bode, A., Schleifer, K.H., 2004. ARB: a software environment for sequence data. *Nucleic Acids Res.* 32, 1363–1371.
- Manera, M., Dezfuli, B.S., 2004. Rodlet cells in teleosts: a new insight into their nature and functions. *J. Fish Biol.* 65, 597–619.
- Mathieu-Daudé, F., Fay, N., Coste, F., Manier, J., Marques, A., Bouix, G., 1992. Occurrence of a in marine cultured gilt-head sea bream from the Languedoc coast: a problem of specificity in the genus *Glugea* (Protozoa, Microspora). *Bull. Eur. Assoc. Fish Pathol.* 12, 67–70.
- Matos, O., Lobo, M.L., Teles, A., Antunes, F., 2004. Is microsporidial infection in animals a potential source for human microsporidiosis? *Southeast Asian J. Trop. Med.* 35, 48–53.
- Matos, O., Lobo, M.L., Xiao, L., 2012. Epidemiology of *Enterocytozoon bieneusi* infection in humans. *J. Parasitol. Res.*, 981424.
- Modin, J.C., 1981. *Microsporidium rhabdophilia* n. sp. from rodlet cells of salmonid fishes. *J. Fish Dis.* 4, 203–211.
- Morrison, J.K., MacConnell, E., Chapman, P.F., Westgard, R.L., 1990. A microsporidium-induced lymphoblastosis in chinook salmon *Oncorhynchus tshawytscha* in freshwater. *Dis. Aquat. Org.* 8, 99–104.
- Mullins, J., Powell, M., Speare, D., Cawthron, R., 1994. An intranuclear microsporidian in lumpfish *Cyclopterus lumpus*. *Dis. Aquat. Org.* 20, 7–13.
- Nilsen, F., Ness, A., Nyland, A., 1995. Observations on an intranuclear microsporidian in lymphoblasts from farmed Atlantic halibut larvae (*Hippoglossus hippoglossus* L.). *J. Eukaryot. Microbiol.* 42, 131–135.
- Nilsen, F., Endresen, C., Hordvik, I., 1998. Molecular phylogeny of microsporidians with particular reference to species that infect the muscles of fish. *J. Eukaryot. Microbiol.* 45, 535–543.

- Nylund, S., Nylund, A., Watanabe, K., Arnesen, C.E., Karlsbakk, E., 2010. *Paranucleospora theridion* n. gen., n. sp. (Microsporidia, Enterocytozoonidae) with a Life Cycle in the Salmon Louse (*Lepeophtheirus salmonis*, Copepoda) and Atlantic Salmon (*Salmo salar*). J. Eukaryot. Microbiol. 57, 95–114.
- Nylund, S., Andersen, L., Saevareid, I., Plarre, H., Watanabe, K., Arnesen, C.E., Karlsbakk, E., Nylund, A., 2011. Diseases of farmed Atlantic salmon *Salmo salar* associated with infections by the microsporidian *Paranucleospora theridion*. Dis. Aquat. Org. 94, 41–57.
- Palenzuela, O., Alvarez-Pellitero, P., Sitjà-Bobadilla, A., 1999. Glomerular disease associated with *Polysporoplasma sparis* (Myxozoa) infections in cultured gilthead sea bream, *Sparus aurata* L. (Pisces: Teleostei). Parasitology 118, 245–256.
- Pruesse, E., Quast, C., Knittel, K., Fuchs, B.M., Ludwig, W., Peplies, J., Glöckner, F.O., 2007. SILVA: a comprehensive online resource for quality checked and aligned ribosomal RNA sequence data compatible with ARB. Nucleic Acids Res. 35, 7188–7196.
- Rastogi, P.A., 2000. MacVector. Integrated sequence analysis for the Macintosh. Methods Mol. Biol. 132, 47–69.
- Refardt, D., Canning, E.U., Mathis, A., Cheney, S.A., Lafranchi-Tristem, N.J., Ebert, D., 2002. Small subunit ribosomal DNA phylogeny of microsporidia that infect Daphnia (Crustacea: Cladocera). Parasitology 124, 381–389.
- Reite, O.B., 2005. The rodlet cells of teleostean fish: their potential role in host defence in relation to the role of mast cells/eosinophilic granule cells. Fish Shellfish Immunol. 19 (253–267), 2005.
- Ronquist, F., Huelsenbeck, J.P., 2003. MrBayes 3: Bayesian phylogenetic inference under mixed models. Bioinformatics 19, 1572–1574.
- Ringø, E., Løvmo, L., Kristiansen, M., Bakken, Y., Salinas, I., Myklebust, R., Olsen, R.E., Mayhew, T.M., 2010. Lactic acid bacteria vs. pathogens in the gastrointestinal tract of fish: a review. Aquac. Res. 41, 451–467.
- Rodríguez-Tovar, L.E., Speare, D.J., Markham, R.J.F., 2011. Fish microsporidia: immune response, immunomodulation and vaccination. Fish Shellfish Immunol. 30, 999–1006.
- Sitjà-Bobadilla, A., Palenzuela, O., 2012. *Enteromyxum* species. In: Woo, P.T.K., Buchmann, K. (Eds.), Fish Parasites: Pathobiology and Protection. CABI Publishing, Oxfordshire (UK) and Cambridge (USA), pp. 163–176.
- Sprague, V., Becnel, J.J., Hazard, E.I., 1992. Taxonomy of phylum microspora. Crit. Rev. Microbiol. 18, 285–395.
- Stentiford, G.D., Bateman, K.S., 2007. *Enterospora* sp., an intranuclear microsporidian infection of hermit crab *Eupagurus bernhardus*. Dis. Aquat. Org. 75, 73–78.
- Stentiford, G.D., Bateman, K.S., Longshaw, M., Feist, S.W., 2007. *Enterospora canceri* n. gen., n. sp., intranuclear within the hepatopancreatocytes of the european edible crab *Cancer pagurus*. Dis. Aquat. Org. 75, 61–72.
- Stentiford, G.D., Bateman, K.S., Dubuffet, A., Chambers, E., Stone, D.M., 2011. *Hepatospora eriocheir* (Wang and Chen, 2007) gen. et comb. nov. infecting invasive Chinese mitten crabs (*Eriocheir sinensis*) in Europe. J. Invert. Pathol. 108, 156–166.
- Stentiford, G.D., Bateman, K.S., Feist, S.W., Chambers, E., Stone, D.M., 2013. Plastic parasites: extreme dimorphism creates a taxonomic conundrum in the phylum Microsporidia. Int. J. Parasitol. 43, 339–352.
- Sveen, S., Overland, H., Karlsbakk, E., Nylund, A., 2012. *Paranucleospora theridion* (Microsporidia) infection dynamics in farmed Atlantic salmon *Salmo salar* put to sea in spring and autumn. Dis. Aquat. Org. 101, 43–49.
- Takvorian, P.M., Buttle, K.F., Mankus, D., Mannella, C.A., Weiss, L.M., Cali, A., 2013. The Multilayered Interlaced Network (MIN) in the sporoplasm of the microsporidium *Annかい algerae* is derived from Golgi. J. Eukaryot. Microbiol. 60, 166–178.
- Tamura, K., Peterson, D., Peterson, N., Stecher, G., Nei, M., Kumar, S., 2011. MEGA5: molecular evolutionary genetics analysis using maximum likelihood, evolutionary distance, and maximum parsimony methods. Mol. Biol. Evol. 28, 2731–2739.
- Tort, L., Padrós, F., Rottlant, J., Crespo, S., 1998. Winter syndrome in the gilthead sea bream *Sparus aurata*. Immunological and histopathological features. Fish Shellfish Immunol. 8, 37–47.
- Tourtip, S., Wongtripop, S., Stentiford, G.D., Bateman, K.S., Sriurairatana, S., Chavadej, J., Sritunyalucksana, K., Withyachumarnkul, B., 2009. *Enterocytozoon hepatopenaei* sp. nov. (Microsporida: Enterocytozoonidae), a parasite of the black tiger shrimp *Penaeus monodon* (Decapoda: Penaeidae): fine structure and phylogenetic relationships. J. Invert. Pathol. 102, 21–29.
- Wongtavatchai, J., Conrad, P.A., Hedrick, R.P., 1995. In vitro characteristics of the microsporidian *Enterocytozoon salmonis*. J. Eukaryot. Microbiol. 42, 401–405.
- Vossbrinck, C.R., Debrunner-Vossbrinck, B.A., 2005. Molecular phylogeny of the microsporidia: ecological, ultrastructural and taxonomic considerations. Folia Parasitol. 52, 131–142.